PEOPLES DEMOCRATIC REPUBLIC OF ALGERIA
MINISTRY OF HIGHER EDUCATION AND SCIENTIFIC RESEARCH

Mohamed Boudiaf University of M'Sila
Faculty of Mathematics and Computer Science
Department of Mathematics

Master memory

Field: Mathematics and Computer Science
Department : Mathematics
Option : Partial Differential Equations and Applications

Theme

Image Processing Based on Fractional Partial Differential Equations

Presented by:
MOUAFAK AZEDINE

Publicly defended on : June 23,2024

In front of the jury composed of:

Benhamidouche Noureddine	Prof ,	M'sila University	**Chairperson**
Chouder Rafaa	M.C.B ,	M'sila University	**Supervisor**
Saadi Abderachid	M.C.A ,	M'sila University	**Examiner**

University year 2023/2024

Contents

Dedication

To my wonderful family,

On this momentous occasion of my graduation, I am overwhelmed with profound gratitude for the unwavering support, boundless love, and endless encouragement you have bestowed upon me throughout my university journey. Today is not just a celebration of my individual achievements but a testament to the remarkable strength and unity that defines our family, I dedicate my graduation to all of you.

Acknowledgments

First of all, I would like to thank "Allah" the all-powerful, for having given us strength and patience since born in this life.

I am grateful to my supervisor, Mr. Chouder Rafaa for their accurate guidance, support, and suggestions that made for this work. Their valuable advice carried me through every stage of writing my memory. It is truly impossible to adequately express my appreciation to them in mere words.

I extend my respect and gratitude to the members of the Jury, Mr. Benhamidouche Noureddine and Mr. Saadi Abderrachid, for graciously agreeing to examine and evaluate my work. Their insightful remarks and suggestions will undoubtedly contribute to enhancing the quality of this memory.

My family, especially my parents, played an indispensable role in the completion of this work. Their unwavering support and encouragement have been invaluable.

Last but not least, I would like to express my gratitude to all my teachers and everyone who has directly or indirectly contributed to the realization of this work.

Introduction

Partial differential equations (PDEs) provide a natural framework for modeling processes in many real-world applications, from physics and life sciences to economics. It is not surprising that they have also significantly contributed to the mathematical foundations of signal and image analysis. For example, they appear as Euler-Lagrange equations when solving continuous optimization problems from variation models [10] or regularizations of ill-posed problems [2]. They are also the natural setting for scale-spaces [1] and are successfully used for image enhancement [17], inpainting [15], and image compression. PDE-based models benefit from decades of research on their theoretical foundations and efficient numerical algorithms. Since they are continuous concepts, it is easy to incorporate useful invariances such as rotation invariance.

One of the most fascinating aspects of PDE-based image analysis is its ability to unify many existing methods in image analysis. This has led to deeper structural insights and novel algorithms. For instance, PDE formulations and their connections to image analysis are well-known for Gaussian smoothing [8], dilation and erosion [4, 16], morphological amoebas [18], mean curvature motion [12], and nonlinear diffusion filtering [14, 5].

Diffusion filtering models are classical methods in image processing. The first step to use linear diffusion for smoothing images was done in the beginning of eighties, when the idea of scale-space filtering has introduced by Witkin [19] and further developed by Koenderink [9]. The linear diffusion filter has its limitations: whether we smooth uniformly by a rotational symmetric Gaussian kernel, or diffuse the data equally in all directions, the process not only removes undesirable local extrema (noise) but also deforms important features of the image, blurs and dislocates edges. To overcome these drawbacks, it have to move to nonlinear filters; nonlinear diffusion offers an excellent alternative.

Nonlinear diffusion has first been proposed for image processing by Perona and Malik in 1990 [14]. This technique not only preserves the edge sharpness, it may also enhance it. However, the Perona-Malik model has several serious practical and theoretical difficulties. Amoung them, for example, To ensure both the existence and uniqueness of solutions, certain conditions must be hold. If these conditions are not satisfied, the process can become unstable; theoretically, the same image could serve as the initial condition for solutions that diverge over time. In this case, Perona and Malik's equation will be an ill-posed problem.

The model which proposed by Catté and .al [5] is a synthesis of Perona and Malik's ideas which avoids the above-mentioned difficulties. As announced by those authors, the main part is devoted to the proof of existence, uniqueness, and regularity properties for the regularized Perona-Malik model. This model has become one of the standard tools for image denoising and simplification in the meantime.

In image processing, integer-order differentiation operators are often used in edge detection, especially, the first order for the gradient and the second order for the Laplacian. However, the first-order derivative methods generally cause thicker edges, resulting in the loss of image details. The second-order derivative methods have a stronger response to fine details, but they are more sensitive to noise. To overcome both inconveniences, there have been introduced fractional-order derivatives.

A fractional derivative is an integral operator that generalizes the ordinary derivative. Fractional derivatives have been used in different areas of science such as anomalous diffusion, circuit theory, image processing, and many others.

Motivated by the above-given ideas and taking into account that the use of fractional derivatives inside the diffusivity function has proven to be effective in edge preservation, authors in [13] proposed a new version of regularized Perona-Malik diffusion using the Caputo-Fabrizio fractional gradient inside the diffusivity function. Experiments showed that filtered images by this new model look better than results with the Perona-Malik filter.

Our aim in this memory is to explore more extensively the model proposed in [13], through a theoretical study that includes an examination of the existence and uniqueness of the solution. In addition, we will conduct a numerical study that allows us to perform numerical experiments to confirm the effectiveness of this model for noise reduction and preserving edges. This will also enable us to compare the obtained results with those of classical models.

The memory is organized as follows: The objective in Chapter (1), is first to present the general concepts of image processing, and also we present basic mathematical concepts that will be used in the next chapters. The second chapter is devoted to the presentation of the famous PDEs that appear in the field of image processing. Starting with the heat diffusion equation, then the Perona-Malik model, and arriving at the regularized Perona-Malik model. In Chapter (3), we presents a fractional diffusion model, which modifies the Perona-Malik model by incorporating the Caputo-Fabrizio fractional gradient into the diffusivity function proposed in [13]. A theoretical investigation will conduct to examine the existence and uniqueness of the solution. Additionally, we will carried out a numerical study, enabling us to perform experiments that confirmed the model's effectiveness in noise reduction and edge preservation. This also allowed us to compare our results with those of the classical Perona-Malik model.

Chapter 1

Preliminaries and Basic Definitions

The goal of this Chapter is to introduce the general concepts of image processing and to present the fundamental mathematical concepts that will be used in the subsequent chapters.

1.1 Introduction to image processing

1.1.1 The image society

In our rapidly evolving world, society can aptly be described as an image society. This designation is not only due to the power and significance of images as a means of communication, but also because of their ease of use, compact nature, and widespread popularity. Images are used by people everywhere to describe, express, and represent the physical world. They capture moments and events, freezing them in time and allowing us to analyse and enhance their quality, highlight specific characteristics, and efficiently combine different pieces of information. From advertising and photography to video games, images permeate our daily lives.
Moreover, there are numerous applications where image processing is integral; almost every area of science and technology can make use of image processing methods. Examples include medical imaging, satellite and aerial imaging, weather forecasting, fingerprint analysis, robotics, quality control, multimedia data management, video processing, and the restoration of old movies, among others (See Figure 1.1). Whether we realize it or not, we are consumers of image processing technology on a daily basis.

1.1.2 Mathematical definition of an image

In image processing, a continuous Gray-scale image is considered that is a two-dimensional function

$$\begin{aligned} u \quad &: \quad \mathbb{R}^2 \to \mathbb{R} \\ &\quad (x, y) \to u(x, y) \end{aligned}$$

The variable (x, y), for digital images, actually belongs to $\mathbb{N}^2$, it is a pixel of the image. $u(x, y)$ represents the luminous intensity, or the Gray level of the image at the pixel (x, y).

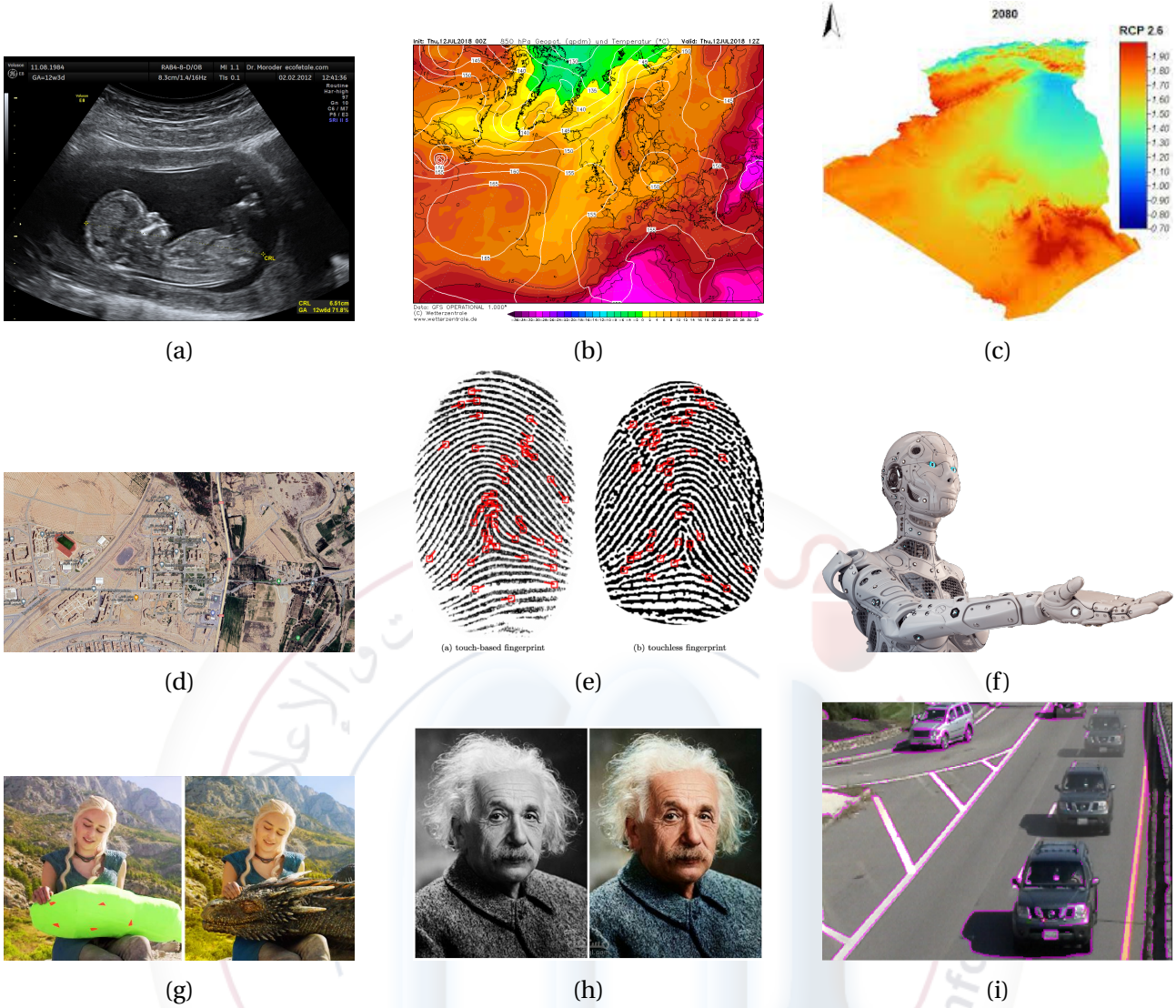

(a) (b) (c)

(d) (e) (f)

(g) (h) (i)

Figure 1.1: Some applications where image processing is concerned.

Digital images are most commonly presented as a matrix of scalars for gray-scale images or vectors for colour images. Digital Gray scale images on the other hand are sampled and quantized. Sampling is the discretization of the image domain. Here an image consists of Gray values of a rectangular point grid $\{u_{i,j} \setminus\ i = 0,...,N-1 \text{ and } j = 0,...,M-1\}$. A grid point (i, j) is called pixel. Here N and M is the width and height of the image in pixels, respectively. $u_{i,j}$ denotes the Gray value of pixel (i, j). (See Figure 1.2).

For a colour image, it is not enough to know its Gray level for each pixel: it is necessary to know the intensity of each of the three channels of the fundamental colours, the red R, the green G, and the blue B. A colour image can then be defined as a vector function, (See Figure 1.3),

$$\begin{aligned} u \quad &: \quad \mathbb{R}^2 \to \mathbb{R}^3 \\ &\quad (x, y) \to u(x, y) = (R(x, y); G(x, y); B(x, y)). \end{aligned}$$

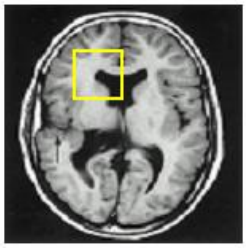

125	131	147	171	173	154	145	128	123
121	124	142	163	169	161	147	135	128
135	131	139	148	155	163	155	144	138
150	150	141	146	150	155	158	157	158
193	189	171	161	162	167	176	182	188
197	207	204	199	198	199	203	205	206
183	202	215	222	219	217	217	214	208
181	198	210	216	218	217	217	37	22
180	197	209	213	216	212	212	91	25
191	201	211	215	214	208	208	21	23
206	208	210	215	215	211	212	16	14

Figure 1.2: Gray level digital image

$RED ==$

124	120	116	116	114	120	125	100	105	128	119
122	117	115	114	112	112	116	89	95	120	113
118	115	113	113	112	111	114	87	93	119	112
120	117	115	116	114	110	113	85	92	117	109
155	155	149	148	152	153	147	141	139	143	147
178	178	173	172	175	180	176	172	170	173	174

$GREEN ==$

145	141	139	139	137	139	142	114	118	141	136
141	138	135	137	135	132	135	106	109	134	132
137	134	133	133	132	136	137	107	112	138	135
139	136	135	136	134	138	138	108	112	137	134
147	147	141	140	144	144	138	132	132	136	140
166	166	161	160	163	167	163	159	160	163	166

$BLUE ==$

150	146	145	145	143	146	150	123	127	150	144
147	143	142	143	141	139	142	114	118	143	139
143	140	140	140	139	141	143	114	119	145	141
145	142	142	143	141	142	143	114	119	144	139
136	136	130	129	133	135	129	123	122	126	130
154	154	149	148	151	158	154	150	150	153	155

Figure 1.3: Color image

1.1.3 What is image processing ?

The goal of image processing and computer vision is to process images in such a way that they are easier to interpret by human beings or better to process by further algorithms. Computer Vision tries to do what a human brain does with the retinal input, it includes understanding and predicting the visual input. That could consist of segmentation, recognition, reconstruction (3D) and prediction (over video data). Classically, many Computer Vision algorithms employed image processing and machine learning or sometimes other methods (e.g Variational Methods, Combinatorial approaches,...) to do the mentioned tasks.
Image processing focuses on enhancing the quality of single images. Image processing algorithms are used for:

- Extraction of important image structures such as edges and corners (since the human visual system is very sensitive to this kind of discontinuities).
- Segmentation: dividing the image into regions of constant color where one has discontinuities at the region boundaries.
- De-blurring: Reconstruction of a visually better image from a blurred image (since in a blurred image edges are smeared and dislocated).
- De-noising: Removing noise from a noisy image.

1.2 Mathematical Background

1.2.1 Functional Spaces

Lebesgue Spaces

We denote by $L^1(\Omega)$ the space of integrable functions from Ω into $\mathbb{R}$.

Definition 1.2.1. *[3] Assume that $p \in \mathbb{R}$ with $1 \leq P < \infty$, we set*

$$L^p(\Omega) = \left\{u : \Omega \to \mathbb{R}; u \text{ is measurable and } |u|^p \in L^1(\Omega)\ ,\right\}$$

with

$$\|u\|_{L^P} = \left(\int_\Omega |u(x)|^p dx\right)^{\frac{1}{P}}$$

.

Definition 1.2.2. *[3] : We set*

$L^\infty(\Omega) = \{u : \Omega \to \mathbb{R}; u \text{ is measurable and there exist a constant } C \text{ such that } |u| \leqslant C \text{ a.e.On } \Omega\}$,

with

$$\|u\|_{L^\infty} = inf\{C; |u(x)| \leqslant c \ \ a.e.\ On\ \ \Omega\}.$$

Remark 1.2.1. *If $f \in L^\infty$ then we have*

$$|u(x)| \leq \|u\|_{L^\infty} \ \ a.e.\ On\ \ \Omega\ .$$

Theorem 1.2.1. *[3] $L^p(\Omega)$ is a vector space and $\|.\|_{L^p}$ is a norm for any p, $1 \leq p \leq \infty$.*

Theorem 1.2.2. *(Fischer-Riesz [3]) L^p is a Banach space for any p, $1 \leq p \leq \infty$.*

Definition 1.2.3. *[7] : Let X denotes a real Banach space with norm $\|\quad\|$. The space $L^p(0,T;X)$, consists of all measurable functions $u : [0,T] \to X$ with*

$$\|u\|_{L^p(0,T;X)} = \left(\int_0^T \|u\|_X^p\right)^{1/p} < \infty,$$

for $1 \leq p < \infty$ and

$$\|u\|_{L^\infty(0,T;X)} = inf\left\{C;\ sup_{0\leq t\leq T}\|u\|_X \leq C\right\}.$$

Definition 1.2.4. *[7] : Let X denotes a real Banach space with norm $\|\quad\|$. The space $C([0,T];X)$, comprises all continuous functions $u : [0,T] \to X$ with*

$$\|u\|_{C([0,T];X)} = max_{0\leq t\leq T}\|u\|_X < \infty.$$

Notation. Let $1 \leq p \leq \infty$; we denote by q the conjugate exponent,

$$\frac{1}{p} + \frac{1}{q} = 1$$

Theorem 1.2.3. *(Young's inequality [7]). Let $1 < p, q < \infty$. Then*

$$ab \leq \frac{a^p}{p} + \frac{b^q}{q},\ (a,b > 0).$$

Theorem 1.2.4. *(Young's inequality with ϵ [7]). Let $1 < p, q < \infty$. Then*

$$ab \leq \epsilon a^p + C(\epsilon) b^q,\ a,b,\epsilon > 0,$$

for $C(\epsilon) = (\epsilon p)^{-q/p} q^{-1}$.

Theorem 1.2.5. *(Höder's inequality [3]). Assume that $f \in L^p(\Omega)$ and $g \in L^q(\Omega)$ with $1 \leq p \leq \infty$. Then, $fg \in L^1(\Omega)$ and*

$$\int_\Omega |fg| \leq \|f\|_{L^p(\Omega)} \|g\|_{L^q(\Omega)}\ .$$

Sobolev Spaces $W^{1,p}(\Omega)$

Definition 1.2.5. *[3]. Let $\Omega \subset \mathbb{R}^N$ be an open set and let $p \in \mathbb{R}$ with $1 \leq p \leq \infty$. The sobolev space $W^{1,p}(\Omega)$ is defined by*

$$W^{1,p}(\Omega) = \left\{ u \in L^p(\Omega) \;\middle|\; \begin{array}{c} \exists g_1, g_2, ..., g_N \in L^p(\Omega) \text{ such that} \\ \int_\Omega u \frac{\partial \phi}{\partial x_i} = -\int_\Omega g_i \phi \;,\; \forall \phi \in C_c^\infty(\Omega) \;,\; \forall i = 1, 2, ..., N \end{array} \right\}$$

We set $H^1(\Omega) = W^{1,2}(\Omega)$.

For $u \in W^{1,p}(\Omega)$ we define $\frac{\partial u}{\partial x_i} = g_i$, and we write

$$\nabla u = \text{grad } u = \left(\frac{\partial u}{\partial x_1}, \frac{\partial u}{\partial x_2}, ..., \frac{\partial u}{\partial x_N} \right).$$

The space $W^{1,p}(\Omega)$ is equipped with the norm

$$\|u\|_{W^{1,p}(\Omega)} = \|u\|_{L^p(\Omega)} + \sum_{i=1}^N \left\| \frac{\partial u}{\partial x_i} \right\|_{L^p(\Omega)}.$$

The space $H^1(\Omega)$ is equipped with the scalar product

$$\langle u, v \rangle_{H^1} = \langle u, v \rangle_{L^2} + \sum_{i=1}^N \left(\frac{\partial u}{\partial x_i}, \frac{\partial v}{\partial x_i} \right)_{L^2} = \int_\Omega uv + \sum_{i=1}^N \int_\Omega \frac{\partial u}{\partial x_i} \frac{\partial v}{\partial x_i}.$$

The associated norm

$$\|u\|_{H^1} = \left(\|u\|_{L^2}^2 + \sum_{i=1}^N \left\| \frac{\partial u}{\partial x_i} \right\|_{L^2}^2 \right)^{1/2}.$$

is equivalent to the $W^{1,2}$ norm.

Proposition 1.2.1. *[3]. $W^{1,p}(\Omega)$ is a Banach space for every $1 \leq p \leq \infty$. $W^{1,p}(\Omega)$ is reflexive for $1 < p < \infty$, and it is separable for $1 \leq p < \infty$. $H^1(\Omega)$ is a separable Hilbert space.*

Theorem 1.2.6. *(Schauder fixed-point theorem [7])*
Suppose that X denotes a real Banach space and $K \subset X$ is compact and convex, and assume also that

$$A : K \to K,$$

is continuous. Then, A has a fixed point in K.

Theorem 1.2.7. *(Grönwall's lemma)*
Let I denote an interval of the real line. Let $v(t)$ and $u(t)$ be real-valued continuous functions defined on I. If $u(t)$ is differentiable in the interior of I and satisfies the differential inequality

$$u'(t) \leq v(t)u(t),$$

then

$$u(t) \leq u(a).exp\left(\int_a^t v(s)ds\right),$$

for all $t \in I$.

1.2.2 Caputo-Fabrizio fractional derivative

Definition 1.2.6. *[6] Let $0 < \alpha < 1$, $u \in H^1$. The Caputo-Fabrizio fractional derivative of order α of a function u is defined by*

$$D^{\alpha}_{0,t}u(t) = \frac{1}{1-\alpha}\int_0^t e^{-\frac{\alpha}{1-\alpha}(t-s)}u'(s)\,\mathrm{d}s \tag{1.1}$$

$$= \frac{1}{1-\alpha}(u(t) - e^{-\frac{\alpha}{1-\alpha}t}u(0)) - \frac{\alpha}{(1-\alpha)^2}\int_0^t e^{-\frac{\alpha}{1-\alpha}(t-s)}u(s)\,\mathrm{d}s \tag{1.2}$$

where u' is the usual derivative of u.

Definition 1.2.7. *[13] Let $0 < \alpha < 1$, $\Omega \subset \mathbb{R}^2$. The fractional gradient of order α, of a function $u : \Omega \to \mathbb{R}$, is defined by*

$$D^{\alpha}u(x,y,t) = (D^{\alpha}_{0x}u(x,y,t), D^{\alpha}_{0y}u(x;y;t)) \tag{1.3}$$

and the module of fractional gradient $|(D^{\alpha}u(x,y,t)|$ is given by

$$|(D^{\alpha}u(x,y,t)| = \sqrt{((D^{\alpha}u(x,y,t))^2 + (D^{\alpha}u(x,y,t))^2}. \tag{1.4}$$

Where $D^{\alpha}_{0,x}u(x,y,t)$ represents the fractional derivative of order α of $u(x,y,t)$ with respect to the variable x and $D^{\alpha}_{0,y}u(x,y,t)$ represents the fractional derivative of order α of $u(x,y,t)$ with respect to the variable y. From the second equality of (1.1), we obtain

$$D^{\alpha}_{0,x}G_{\sigma}(x,y) = \frac{1}{1-\alpha}\int_0^x e^{-\frac{\alpha}{1-\alpha}(x-\tau)}\frac{\partial G_{\sigma}(\tau,y)}{\partial\tau}\,\mathrm{d}\tau$$

$$= \frac{1}{1-\alpha}(G_{\sigma}(x,y) - e^{-\frac{\alpha}{1-\alpha}x}G_{\sigma}(0,y)) - \frac{\alpha}{(1-\alpha)^2}\int_0^x e^{-\frac{\alpha}{1-\alpha}(x-\tau)}G_{\sigma}(\tau,y)\,\mathrm{d}\tau$$

and

$$D^{\alpha}_{0,y}G_{\sigma}(x,y) = \frac{1}{1-\alpha}\int_0^y e^{-\frac{\alpha}{1-\alpha}(y-\tau)}\frac{\partial G_{\sigma}(x,\tau)}{\partial\tau}\,\mathrm{d}\tau$$

$$= \frac{1}{1-\alpha}(G_{\sigma}(x,y) - e^{-\frac{\alpha}{1-\alpha}y}G_{\sigma}(x,0)) - \frac{\alpha}{(1-\alpha)^2}\int_0^y e^{-\frac{\alpha}{1-\alpha}(y-\tau)}G_{\sigma}(x,\tau)\,\mathrm{d}\tau$$

1.2.3 Finite difference approximations

When a function U and its derivatives are single-valued, finite and continuous functions of x, then by Taylor's theorem,

$$U(x+h) = U(x) + hU'(x) + \frac{1}{2}h^2U''(x) + \frac{1}{6}h^3U^{(3)}(x) + \frac{1}{4!}h^4U^{(4)}(x) + \ldots \tag{1.5}$$

and

$$U(x-h) = U(x) - hU'(x) + \frac{1}{2}h^2u''(x) - \frac{1}{6}h^3U^{(3)}(x) + \frac{1}{4!}h^4U^{(4)}(x) + \ldots \tag{1.6}$$

Addition of these expansions gives

$$U(x+h)+U(x-h)=2U(x)+h^2U''(x)+O\left(h^4\right)$$

where $O\left(h^4\right)$ denotes terms containing fourth and higher powers of h. Assuming these are negligible in comparison with lower powers of h it follows that,

$$U''(x)=\left(\frac{\mathrm{d}^2U}{\mathrm{d}x^2}\right)_{x=x}\approx\frac{1}{h^2}\{U(x+h)-2U(x)+U(x-h)\} \tag{1.7}$$

with a leading error on the right-hand side of order h^2.

Subtraction of Eq. (1.6) from Eq. (1.5) and neglect of terms of order h^3 leads to

$$U'(x)=\left(\frac{\mathrm{d}U}{\mathrm{d}x}\right)_{x=x}\approx\frac{1}{2h}\{U(x+h)-U(x-h)\} \tag{1.8}$$

with an error of order h^2. Equation (1.8) clearly approximates the slope of the tangent at the point P by the slope of the chord AB, and is called a central-difference approximation (Figure 1.4). We can also approximate the slope of the tangent at P by either the slope of the chord PB, giving the forward-difference formula,

$$U'(x)\approx\frac{1}{h}\{U(x+h)-U(x)\},$$

or the slope of the chord AP giving the backward-difference formula,

$$U'(x)\approx\frac{1}{h}\{U(x)-U(x-h)\},$$

with an error of order h.

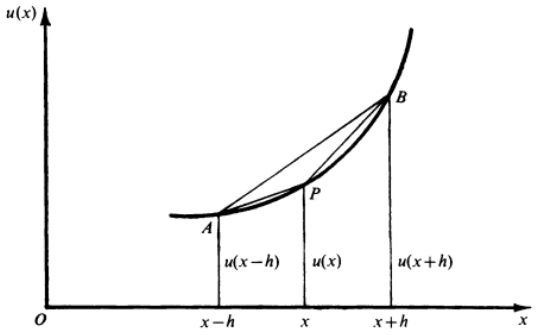

Figure 1.4: Approximations of the slope of the tangent at point P by the slope of the chord AB, and by the slope of the chord PB.

Notation for functions of several variables:

Assume U is a function of the independent variables x and t. Subdivide the $x-t$ plane into sets of equal rectangles of sides $\Delta x=h,\Delta t=k$, by equally spaced grid lines parallel to Oy, defined by $x_i=$

ih, $i = 0, \pm 1, \pm 2, \ldots$, and equally spaced grid lines parallel to Ox, defined by $t_j = jk$, $j = 0, 1, 2, \ldots$, as shown in figure 1.5. Denote the value of U at the representative mesh point $P(ih, jk)$ by

$$U_{i,j} = U(ih, jk).$$

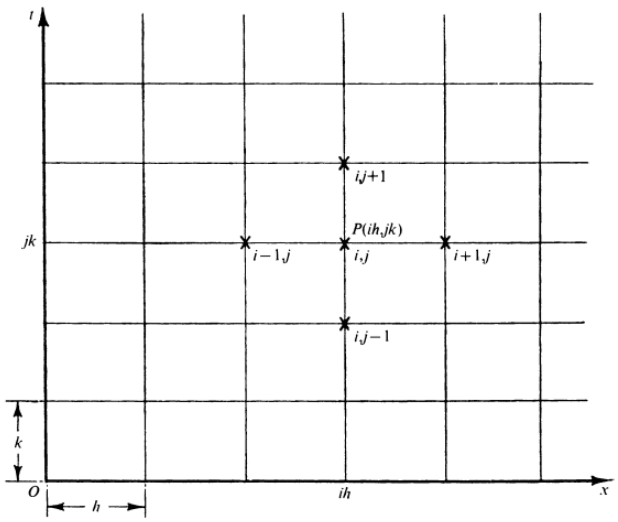

Figure 1.5: Approximated value of U at the representative mesh point P.

Then by Eq.(1.7),

$$\left(\frac{\partial^2 U}{\partial x^2}\right)_{i,j} \approx \frac{U\{(i+1)h, jk\} - 2U\{ih, jk\} + U\{(i-1)h, jk\}}{h^2}.$$

i.e.

$$\left(\frac{\partial^2 U}{\partial x^2}\right)_{i,j} \approx \frac{U_{i+1,j} - 2U_{i,j} + U_{i-1,j}}{h^2},$$

with a leading error of order h^2.

With this notation the forward (resp. backward) difference approximation for $\partial U/\partial x$ at P is

$$\left(\frac{\partial U}{\partial x}\right)^{+}_{i,j} \approx \frac{U_{i+1,j} - U_{i,j}}{h}, \left(\frac{\partial U}{\partial x}\right)^{-}_{i,j} \approx \frac{U_{i,j} - U_{i-1,j}}{h},$$

with a leading error of $O(h)$.

The forward-difference approximation for $\partial U/\partial t$ at P is

$$\frac{\partial U}{\partial t} \approx \frac{U_{i,j+1} - U_{i,j}}{k},$$

with a leading error of $O(k)$.

Chapter 2

PDEs in image processing

This Chapter is devoted to the presentation of the famous PDEs that appear in the field of image processing. Starting with the heat diffusion equation, then the Perona-Malik model, and arriving at the regularized Perona-Malik model.

2.1 Linear diffusion filtering (Heat equation)

The first step to use PDEs for smoothing images was done in the beginning of eighties, when the idea of scale-space filtering has introduced by Witkin [19] and further developed by Koenderink [9].

The essential idea of this approach is quite simple: embed the original image in a family of derived images $u(x,t)$ obtained by convolving the original image u_0 with a Gaussian kernel $G_{\sqrt{2t}}(x)$ of variance t:

$$u(x,t) = \left(G_{\sqrt{2t}} * u_0\right)(x),$$

where

$$G_\sigma(x) = C\sigma^{-1/2} exp\left(-|x|^2/4\sigma\right).$$

This family of derived images may equivalently be viewed as the solution of the following heat equation or the linear diffusion equation:

$$\begin{cases} \frac{\partial u(x,t)}{\partial t} &= \Delta u(x,t) \qquad \text{for } t>0 \text{ and } x \in \Omega \\ u(x,0) &= u_0(x) \qquad \text{for } x \in \Omega \end{cases} \tag{2.1}$$

for a function $u(x,t)$ is the smoothed image at t, and Δ denote Laplacian operator, with the initial condition $u(x,0) = u_0(x)$, is the original image. $\Omega \subset \mathbb{R}^2$.

Koenderink [9] motivates the diffusion equation formulation by stating two criteria:

- **Causality:** Any feature at a coarse level of resolution is required to possess a (not necessarily unique) "cause" at a finer level of resolution although the reverse need not be true. In other words, no spurious detail should be generated when the resolution is diminished.
- **Homogeneity and Isotropy:** The blurring is required to be space invariant.

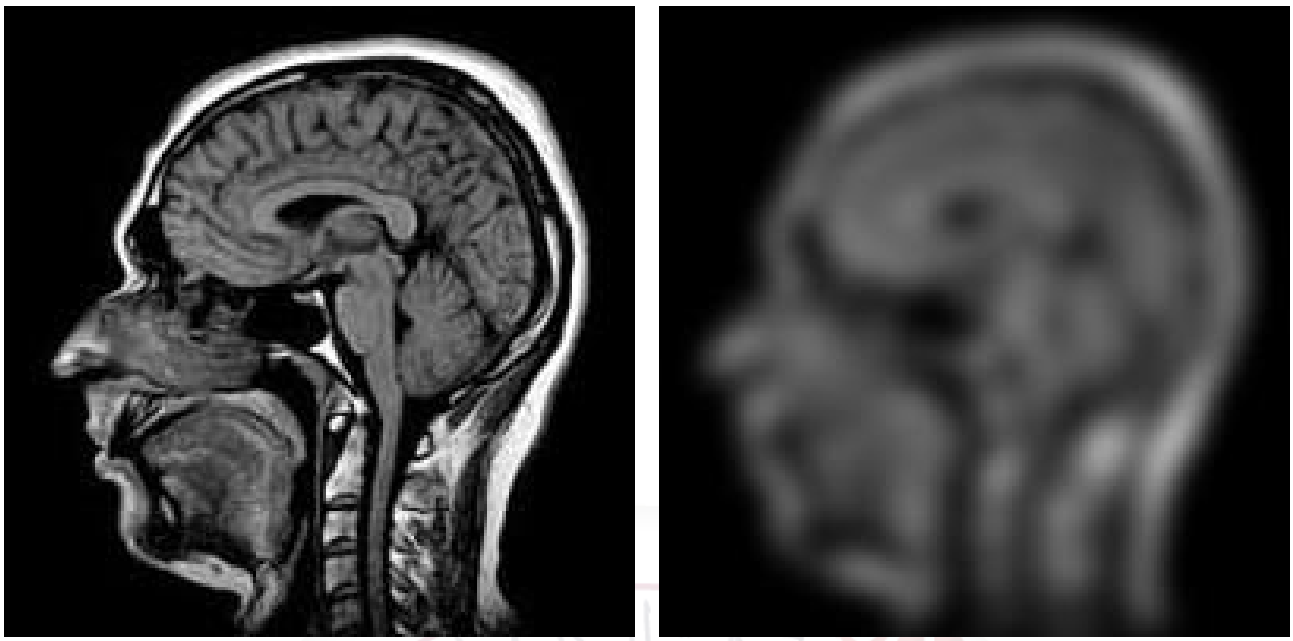

(a) (b)

Figure 2.1: Gray-scale image (a) and its filtered version by linear diffusion filtering (b).

The linear diffusion filter has its limitations: whether we smooth uniformly by a rotational symmetric Gaussian kernel, or diffuse the data equally in all directions, the process not only removes undesirable local extrema (noise) but also deforms important features of the image, blurs and dislocates edges (See Figure 2.1). To overcome these drawbacks, we have to move to non-linear filters; non-linear diffusion offers an excellent alternative.

2.2 Non-linear diffusion filtering (Perona-Malik model)

Overcoming the undesirable effects of linear smoothing filtering, such as blurring or dislocating the semantically meaningful edges of the image, non-linear diffusion equations can be used because the non-linear diffusion technique not only preserves the edge sharpness, it may also enhance it. An important improvement of the edge detection theory has been introduced by Perona and Malik [14], by stating three criteria:

- **Causality:** no spurious detail should be generated passing from finer to coarser scales.
- **Immediate localization:** boundaries should be sharp and coincide with the semantically meaningful boundaries at that resolution.
- **Piecewise smoothing:** intra-region smoothing should be preferred to inter-region smoothing.

To satisfy the second and third criteria, Perona and Malik propose to replace the heat equation by a non-linear equation of the porous medium type:

$$\begin{cases} \frac{\partial u(x,t)}{\partial t} & = div\left(g\left(|\nabla u|\right)\nabla u\right) \quad \text{for } t>0 \text{ and } x\in\Omega \\ u(x,0) & = u_0(x) \quad \text{for } x\in\Omega \end{cases} \tag{2.2}$$

In this equation, g is a smooth non-increasing function with $g(0)=1$, $g(s)\geq 0$, and $g(s)$ tending to zero at infinity. The idea is that the smoothing process obtained by the equation is "conditional": if $\nabla u(x)$ is large, then the diffusion will be low and therefore the exact localization of the "edges" will be kept. Conversely, if $\nabla u(x)$ is small, then the diffusion will tend to smooth still more around x. Thus the choice of g corresponds to a sort of thresholding which has to be compared to the thresholding of $|\nabla u|$ used in the final step of the classical theory. Since this thresholding introduces a nonlinear device anyway, it was natural to ask whether it could not be used earlier in the method, in the smoothing process itself.

Nonlinear diffusion filtering can successfully smooth noise while respecting the region boundaries and small structures within the image, as long as some of its crucial parameters are determined or estimated correctly. According to Perona and Malik, the choice of functions g which satisfies some properties leads to the desirable result of edge enhancement.

The experimental results obtained by Perona and Malik are perceptually impressive and show that an "edge detector" based on this theory gives edges which remain much more stable across the scales. (This property has been sought by many researchers in the past two decades).

For a useful comparison between the linear and nonlinear diffusion filtering methods and their impact on edge sharpness, an example for a gray-scale image filtred by linear and nonlinear diffusion is given in Figure 2.2.

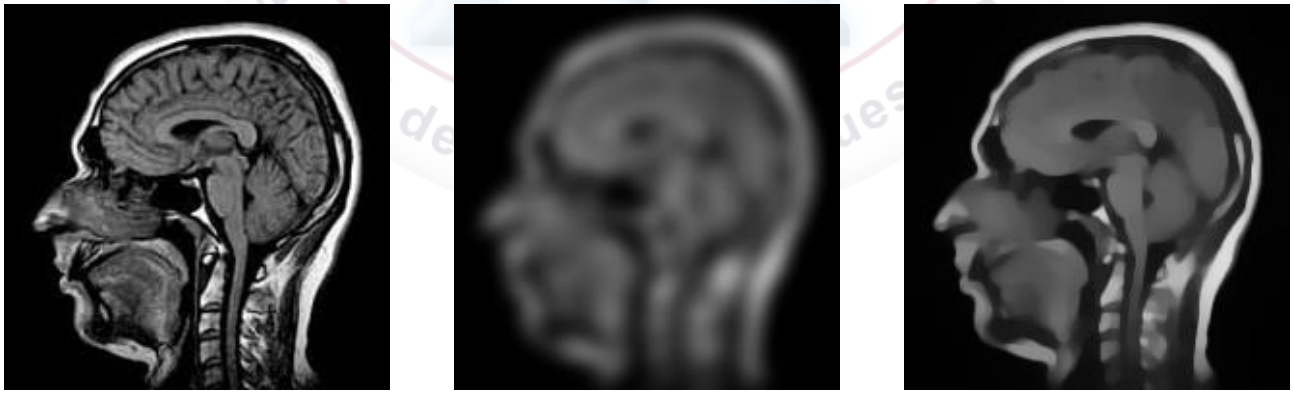

(a) (b) (c)

Figure 2.2: Gray-scale image and its filtered versions. (a) Original image. (b) Linear diffusion filtering. (c) Nonlinear diffusion filtering.

As seen in Figure 2.2, the linear diffusion filtering blurs the edge, whereas the nonlinear diffusion filtering preserves edge sharpness.

However, the Perona-Malik model has several serious practical and theoretical difficulties.

- The first is a straightforward objection that every researcher in signal analysis will surely raise (and that Malik and Perona themselves considered). Assume that the signal is noisy, with white noise, for instance. Then the noise introduces very large, in theory unbounded, oscillations of the gradient ∇u. Thus the conditional smoothing introduced by the model will not help, since all these noise edges will be kept !

  Perona and Malik proposed to eliminate this difficulty by a first smoothing of the image using some low pass filter. It seems to work well in practice, but it is nonetheless a trick which should be avoided in a correct theory. An obvious drawback is the introduction in the method of a new parameter, the variance of the Gaussian with which this preliminary smoothing should be made. Moreover, the theory seems to adopt again what it tried to avoid: a non-adaptive filtering which makes lost the accuracy of the edges.

- The second difficulty arises from the equation itself; among the functions g which Perona and Malik consider admissible are found functions of the type $g(s) = e^{-s}$ or $g(s) = (1+s^2)^{-1}$ for which no correct theory of (2.2) is available. Indeed, in order to obtain both existence and uniqueness of the solutions, g must verify that $sg(s)$ is non-decreasing. If this condition is not verified, we can observe for some functions g with $sg(s)$ non-increasing a nondeterministic and therefore unstable process; the same picture in theory can be the initial condition of solutions divergent in time. In practice, that means that very close pictures can produce divergent solutions and therefore different edges. This is certainly a drawback for most applications. If $sg(s)$ is non-increasing, Perona and Malik's equation will be an ill-posed problem.

Before arriving at an improved model, let us just sketch why, if $sg(s)$ is non increasing, Perona and Malik's equation will be an ill-posed problem.

Without loss of generality, take the case where the signal is one-dimensional. The equation becomes

$$\frac{du}{dt} - (g(u')u')' = 0,$$

that is,

$$\frac{du}{dt} - (g'(u')u' + g(u'))u'' = 0.$$

If $sg(s)$ is decreasing at some s and therefore with a negative derivative $-a$ at s, and if it happens that at some point x, $u'(x) = s$, then the equation looks near x like

$$\frac{du}{dt} + au'' = 0.$$

This is the inverse heat equation, which actually is known to be ill-posed; starting with a smooth initial datum, it can develop singularities of any order in arbitrarily small time.

2.3 Regularization of Perona-Malik model

The model which proposed by Catté and .al [5] is a synthesis of Perona and Malik's ideas which avoids the above-mentioned difficulties; it will be robust in the presence of noise and will be consistent from the formal viewpoint described above. Moreover, it will be based, as in the space scale theory of Witkin, on a single parameter: the scale.

It can define the "selective smoothing" of u_0 at scale $\sqrt{t}$ as the function $u(x,t)$ verifying

$$\begin{cases} \frac{\partial u(x,t)}{\partial t} & = div\left(g\left(|\nabla G_\sigma * u|\right)\nabla u\right) \quad \text{for } t>0 \text{ and } x\in\Omega \\ u(x,0) & = u_0(x) \quad \text{for } x\in\Omega \end{cases} \tag{2.3}$$

where $G_\sigma(X) = C\sigma^{-1/2}exp(-|X|^2/4\sigma)$. As mentioned in section (2.1), it is easily seen that $G(x,t) = G_t(x)$ is nothing but the fundamental solution of the heat equation. Therefore, the term $(DG_\sigma * u)(x,t)$ which appears inside the divergence term of 2.3 is simply the gradient of the solution at time σ of the heat equation with $u(x,t)$ as initial datum. Thus it appears to be an estimate of the gradient of u at point x. The modification of the model of Perona and Malik, therefore, is only to replace the gradient $|\nabla u|$ by its estimate $|DG_\sigma * u|$. According to Catté and al. [5], this slight change of the model is enough to avoid both inconsistencies of the Perona and Malik model. Indeed, the equation, as announced by those authors, will now diffuse if and only if the gradient is estimated to be small, the job of this estimate being done by the new term which we introduce. This does not alter the scope of the "anisotropic diffusion" model. Indeed, the initial datum in the new equation is u_0, and the necessity of smoothing the initial datum u_0 by a Gaussian in order to eliminate the noisy estimates of $|\nabla u|$ is now removed. Additionally, 2.3 is proven to have a unique smooth solution. The main focus of Catté and al.'s work is proving the existence, uniqueness, and regularity properties of 2.3.

The function G to be considered can be any "low pass filter", or, to use the terminology of calculus, any smoothing kernel. However, in order to preserve the notion of scale in the gradient estimate, it is convenient that this kernel depends on a scale parameter. A good and classical example is, as mentioned above, the Gaussian. It is important to keep this particular case in mind. Indeed, a question which arises immediately in the consideration of model 2.3 is what time is best for "stopping" the evolution of the signal $u(x,t)$. This choice is quite important, since it is clear that all of the above-mentioned models, diffuse completely at $t\to+\infty$ and give therefore a constant function. Now we may appeal to the Witkin model to answer this question: according to this model, time is interpreted as a "scale factor." (More precisely, the solution $u(x,t)$ at time t corresponds to a scale $\sqrt{t}$. Indeed, roughly speaking, $u(x,t)$ appears in the Witkin model as a smooth version of u_0 obtained by convolving it with a filter of spatial width $\sqrt{t}$.) Thus in the model 2.3 it is coherent to correlate the stopping time t and the time introduced via the estimator G_σ. We should therefore choose a stopping time t of the order of σ. Then the spatial scale under which the signal

is smoothed in regular zones of the image will be of the order of $\sqrt{t}$. On the parts of the picture where edges are present, the situation is different.

Since the scope of the equation 2.3 is to delay diffusion in these zones, the scale at which edge information is lost will depend on the shape of the thresholding function g. Therefore, even if we wrote above that we should stop the equation at a time of the order of σ, this is rather a lower estimate and there is no inconsistency in looking at what happens to the signal $u(x,t)$ for times greater than σ. In experimentation, it might be convenient to play with two parameters that are anyway at hand in any edge detection model: the scale parameter (spatial width of the filtering) on the one side, $\sqrt{\sigma}$. and the threshold parameter for edges, which is implicit in the shape of g. If g is near 1 on some interval containing zero and decreases briskly at the end λ of this interval, then λ is the threshold for edges. Where $|\nabla u|$ is greater than λ, the edges will remain and where it is smaller, they will disappear. Thus it is clear that if the regularized Perona-Malik model is used as a preliminary step for an edge detection device, we might use the same threshold λ on the gradient for keeping the edges as the one implicit in g.

Theorem 2.3.1. *[5] Let $u_0 \in L^2(\Omega)$, there exists a unique function $u(x,t)$ such that $u \in \mathscr{C}\left([0,T];L^2(\Omega)\right) \cap L^2(0,T,H^1(\Omega))$, and verifying*

$$\frac{\partial u}{\partial t} = div[g(|\nabla G_\sigma * u|)\nabla u] \qquad in\ ]0,T]\times\Omega \tag{2.4}$$

$$\frac{\partial u}{\partial n} = 0, \qquad on\ \partial\Omega\times]0,T] \tag{2.5}$$

$$u(0) = u_0 \qquad in\ \Omega \tag{2.6}$$

where this system is verified in the distributional sense. Moreover, this unique solution is in $\mathscr{C}^\infty\left(]0,T[\times\bar{\Omega}\right)$.

Numerical schemes

By simply using the finite differences introduced above, one way of discretising the right terms in (2.4) is using the central difference. First we apply the central difference and then the forward and the backward differences for approximating the corresponding derivatives.

Discretisation of div Operator

Now that we know how to approximate first and second order derivatives, we can discretise the divergence, div, operator. Conceptually, we have two different cases:

$$\begin{gathered}\operatorname{div}(\nabla f)\\ \operatorname{div}(g(x,y,t)\nabla f)\end{gathered} \tag{2.7}$$

Here, physical interpretation of the divergence is, in a sense, that of diffusion . In the case of $div(\nabla f)$, diffusivity is the same in each direction, whereas in the case of $div(g(x,y,t)\nabla f)$, diffusivity is defined (or controlled) by the function g and is not necessarily the same in all the directions.

Mathematically, for a differentiable vector function $F = U\vec{i} + V\vec{j}$, divergence operator is defined as:

$$div(F) = \frac{\partial U}{\partial x} + \frac{\partial V}{\partial y} \tag{2.8}$$

In other words, divergence is a sum of partial derivatives of a differentiable vector function. Therefore, in our case, we have the following.

$$\begin{aligned} div(\nabla f) &= \frac{\partial}{\partial x}\left(f_x\right) + \frac{\partial}{\partial y}\left(f_y\right) = \frac{\partial^2 f}{\partial x^2} + \frac{\partial^2 f}{\partial y^2} = \Delta f \\ div(g(x,y,t)\nabla f) &= \frac{\partial}{\partial x}\left(g(x,y,t) f_x\right) + \frac{\partial}{\partial y}\left(g(x,y,t) f_y\right) = \nabla g \cdot \nabla f + g\Delta f \end{aligned} \tag{2.9}$$

Now, by simply using the finite differences introduced above, one way of discretising the divergence terms in (2.9) is using the central difference. First we apply the central difference and then the forward- and the backward differences for approximating the corresponding derivatives. The 'trick' here is to realise that $\left(f_x\right)(x+\frac{1}{2}, y)$ is actually the forward difference $D_x^+ f(x)$, while $\left(f_x\right)(x-\frac{1}{2}, y)$ is the backward difference $D_x^- f(x)$. Equations (2.10) , and (2.11) show the discretisation for $div(\nabla f)$, and $div(g(x,y,t)\nabla f)$, respectively. This is the same discretisation as in the famous paper by Perona and Malik.

$$\begin{aligned} \frac{\partial}{\partial x}\left(f_x\right)(x,y) + \frac{\partial}{\partial y}\left(f_y\right)(x,y) &= \left(f_x\right)(x+\frac{1}{2}, y) - \left(f_x\right)(x-\frac{1}{2}, y) \\ &\quad + \left(f_y\right)(x, y+\frac{1}{2}) - \left(f_y\right)(x, y-\frac{1}{2}) \\ &= f(x+1,y) - f(x,y) + f(x-1,y) - f(x,y) \\ &\quad + f(x,y+1) - f(x,y) + f(x,y-1) - f(x,y) \\ &= \nabla_E f + \nabla_W f + \nabla_S f + \nabla_N f \end{aligned} \tag{2.10}$$

where $\nabla_{\{W,N,E,S\}} f$ denotes the difference in the directions given by W, N, E, S.

As it was already mentioned, first we apply first order central difference on $f_x(x,y)$, and thus obtain

$$\begin{aligned} \frac{\partial}{\partial x}\left(g f_x\right)(x,y) + \frac{\partial}{\partial y}\left(g f_y\right)(x,y) &= \left(g f_x\right)(x+\frac{1}{2}, y) - \left(g f_x\right)(x-\frac{1}{2}, y) \\ &\quad + \left(g f_y\right)(x, y+\frac{1}{2}) - \left(g f_y\right)(x, y-\frac{1}{2}) \\ &= g(x+\frac{1}{2}, y)(f(x+1,y) - f(x,y)) \\ &\quad + g(x-\frac{1}{2}, y)(f(x-1,y) - f(x,y)) \\ &\quad + g(x, y+\frac{1}{2})(f(x,y+1) - f(x,y)) \\ &\quad + g(x, y-\frac{1}{2})(f(x,y-1) - f(x,y)) \\ &= g_E \nabla_E f + g_W \nabla_W f + g_S \nabla_S f + g_N \nabla_N f \end{aligned} \tag{2.11}$$

where $g_{\{W,N,E,S\}}$ denotes diffusivity in the directions given by W, N, E, S. As it can be observed from Equation (2.11), we need to approximate the diffusivity between the pixels. A simple '2-point'

approximation would be the average between neighbouring pixels, for example

$$g(x+\frac{1}{2},y)=[g(x+1,y)+g(x,y)]/2.$$

As it was already mentioned above, physical interpretation of the divergence is, in a sense, diffusion: the divergence operator introduces a 'connectivity' between the pixels. This simply means, as will be shown later on, that a solution at any position (i,j) will depend on the solution at neighbouring positions. Because of this kind of a dependency of the solution between the adjacent positions, variational correspondence methods are said to be 'global'.

Discretised Diffusion Equation

In order to solve Equation (2.4) of explicit scheme we need to discretise the divergence operator. We start by marking the positions of the pixels of interest with (i,j) :

$$\frac{u_{i,j}^{t+1}-u_{i,j}^{t}}{\Delta t}=\operatorname{div}\left(g^{t}\nabla u^{t}\right)$$

After this we discretise the div operator, as given by Equation (2.11), and obtain the following:

$$\begin{aligned}u_{i,j}^{t+1}-u_{i,j}^{t}=&\Delta t g_{N}^{t}\left(u_{i-1,j}^{t}-u_{i,j}^{t}\right)\\&+\Delta t g_{S}^{t}\left(u_{i+1,j}^{t}-u_{i,j}^{t}\right)\\&+\Delta t g_{W}^{t}\left(u_{i,j-1}^{t}-u_{i,j}^{t}\right)\\&+\Delta t g_{E}^{t}\left(u_{i,j+1}^{t}-u_{i,j}^{t}\right)\end{aligned}\tag{2.12}$$

The only thing left to do, is arrange the terms:

$$\begin{aligned}u_{i,j}^{t+1}=&u_{i,j}^{t}\left(1-\Delta t\left(g_{N}^{t}+g_{S}^{t}+g_{W}^{t}+g_{E}^{t}\right)\right)\\&+\Delta t g_{N}^{t}\left(u_{i-1,j}^{t}\right)+\Delta t g_{S}^{t}\left(u_{i+1,j}^{t}\right)+\Delta t g_{W}^{t}\left(u_{i,j-1}^{t}\right)+\Delta t g_{E}^{t}\left(u_{i,j+1}^{t}\right)\end{aligned}\tag{2.13}$$

Experimental results

In this section, we will discuss the influence of the model (2.4) on a diverse range of gray scale images. Figures (2.3 and 2.4) show how noise reduction and edge preservation can be combined using this model.

(a) (b) (c)

Figure 2.3: Gray-scale image and its filtered versions. (a) Original image. (b) Smoothed image by Perona-Malik model. (c) Smoothed image by regularized Perona-Malik model.

(a) (b) (c)

Figure 2.4: (a) Original image. (b) Denoised image by Perona-Malik model. (c) Denoised image by regularized Perona-Malik model.

Chapter 3

Perona-Malik model with diffusion coeficient depending on fractional gradiant

This chapter presents a fractional diffusion model, which modifies the Perona-Malik model by incorporating the Caputo-Fabrizio fractional gradient into the diffusivity function proposed in [13]. A theoretical investigation will conduct to examine the existence and uniqueness of the solution. Additionally, we will carried out a numerical study, enabling us to perform experiments that confirmed the model's effectiveness in noise reduction and edge preservation.

3.1 Existence and unicity

In this section, we establish the existence and uniqueness of the following problem

$$\frac{\partial u(t)}{\partial t} - div[g(|(D^\alpha G_\sigma) * u|)\nabla u] = 0 \qquad \text{in } \Omega \times [0,T] \tag{3.1}$$

$$\frac{\partial u}{\partial n} = 0, \qquad \text{on } \partial\Omega \times [0,T] \tag{3.2}$$

$$u(0) = u_0 \qquad \text{in } \Omega \tag{3.3}$$

where Ω is a bounded domain of $\mathbb{R}^2$ with an appropriately smooth boundary, n denotes the unit outer normal to Ω, and $T > 0$. To facilitate the analysis, we consider the weak formulation of the problem. We seek a function $u \in \mathscr{C}([0,T]; L^2(\Omega) \cap L^2(0,T; H^1(\Omega))$ such that for all test functions $v \in H^1(\Omega)$,

$$\begin{aligned} < \frac{\partial u(t)}{\partial t}, v > &= < div[g(|(D^\alpha G_\sigma) * u|)\nabla u], v > \\ &= \int_\Omega div[g(|(D^\alpha G_\sigma) * u|)\nabla u]\, v \, dx, \end{aligned}$$

integrating by parts,

$$\int_\Omega div[g(|(D^\alpha G_\sigma) * u|)\nabla u]\, v \, dx = \int_\Omega \frac{\partial}{\partial n}(g(|(D^\alpha G_\sigma) * u|)\nabla u)\, v \, ds - \int_\Omega g(|(D^\alpha G_\sigma) * u|)\nabla u \nabla v \, dx,$$

using the Neumann boundary condition (3.2), we obtain

$$< \frac{\partial u(t)}{\partial t}, v > + \int_\Omega g(|(D^\alpha G_\sigma) * u|)\nabla u \nabla v \, dx = 0 \qquad \forall v \in H^1(\Omega)$$

$$u(0) = u_0$$

Theorem 3.1.1. *[13] Let $u_0 \in L^2(\Omega)$, there exists a unique function $u(x,t)$ verifying (3.1)-(3.2) such that $u \in \mathscr{C}([0,T];L^2(\Omega) \cap L^2(0,T;H^1(\Omega))$.*

To prove this theorem, we first start with the following Lemma.

Lemma 3.1.1. *Let $\Omega \subset R^2$ and $u \in L^2(\Omega)$, then there exists a constant $C_1 > 0$ such that*

$$||(D^\alpha G_\sigma) * u||_{L^\infty(\Omega)} \leq C_1 ||u||_{L^2(\Omega)}. \tag{3.4}$$

Moreover, there exists a constant $C_2 > 0$, such that

$$||g(|(D^\alpha G_\sigma) * u|) - g(|(D^\alpha G_\sigma) * v|)||_{L^\infty(\Omega)} \leq C_2 ||u - v||_{L^2(\Omega)}. \tag{3.5}$$

Proof: We have

$$\begin{aligned} |(D^\alpha G_\sigma) * u| &\leq \int_\Omega |(D^\alpha G_\sigma)(x-y)u(y)|dy \\ &= \int_\Omega |(D^\alpha G_\sigma)(x-y)|.|u(y)|dy \end{aligned} \tag{3.6}$$

Since $u \in L^2(\Omega)$, then from (3.6) we obtain

$$|(D^\alpha G_\sigma) * u| \leq C_1 ||u||_{L^2(\Omega)}, \tag{3.7}$$

Moreover, since $g(s)$ and $(D^\alpha G\sigma) * u$ are smooth, then $g(|D^\alpha G\sigma * u|)$ is smooth. Therefore $g(|D^\alpha G\sigma * u|)$ is Lipchitz continuous function. Indeed

$$\begin{aligned} &||g(|(D^\alpha G_\sigma) * u|) - g(|(D^\alpha G_\sigma) * v|)||_{L^\infty(\Omega)} \\ &\leq C|||(D^\alpha G_\sigma) * u| - |(D^\alpha G_\sigma) * v|||_{L^\infty(\Omega)} \\ &\leq C|||(D^\alpha G_\sigma) * u - (D^\alpha G_\sigma) * v|||_{L^\infty(\Omega)} \\ &= C|||(D^\alpha G_\sigma) * (u - v)|||_{L^\infty(\Omega)} \\ &\leq C||C||u - v||_{L^2(\Omega)}||_{L^\infty(\Omega)} \\ &\leq C_2 ||u - v||_{L^2(\Omega)} \end{aligned}$$

which implies (3.4).

3.1.1 Existence

We consider the proof of the existence, which is based on Schauder fixed-point theorem. Firstly, we introduce the space

$$W(0,T) = \left\{ \omega \in L^2(0,T;H^1(\Omega)), \frac{\partial \omega}{\partial t} \in L^2(0,T;(H^1(\Omega))') \right\}$$

This space is a Hilbert space ([5]). Let $\omega \in W(0,T) \bigcap L^{\infty}(0,T;L^2(\Omega))$ such that

$$||\omega||_{L^{\infty}(0,T;L^2(\Omega))} \leq ||u_0||_{L^2(\Omega)}, \tag{3.8}$$

and

$$\left|\left|\frac{\partial \omega}{\partial t}\right|\right|_{L^2(0,T;(H^1(\Omega))'} \leq ||u_0||_{H^1(\Omega)} \tag{3.9}$$

Let now consider the following linear problem (P_w):

$$< \frac{\partial u(t)}{\partial t}, v > + \int_{\Omega} g(|D^{\alpha} G_{\sigma}) * \omega|) \nabla u(t) \nabla v(t) \, dx = 0 \qquad \forall v \in H^1(\Omega) \tag{3.10}$$

$$u(0) = u_0 \tag{3.11}$$

which, according to the classical results on parabolic equations [7], has a unique solution. Since ω and $\partial\omega(t)/\partial t$ satisfy (3.8) and (3.9) respectively, then $|(D^{\alpha} G_{\sigma}) * \omega|$ and $|(D^{\alpha} G_{\sigma}) * (\partial\omega(t)/\partial t)$ belong to $L^{\infty}((0,T);\mathscr{C}^{\infty}(\Omega))$ and there exists a constant $M = M(G_{\sigma}, ||u_0||_{H^1(\Omega)})$ such that $|(D^{\alpha} G_{\sigma}) * \omega| \leq M$ and $|(D^{\alpha} G_{\sigma}) * \omega(t)/\partial t| \leq M$, for al $x \in \Omega$. Since g is decreasing and positive, there exists a constant $\nu > 0$ such that

$$1 \geq g(|(D^{\alpha} G_{\sigma}) * w|) \geq \nu \tag{3.12}$$

Proposition 3.1.1. *The problem (P_w) has a unique solution $u_{\omega} \in W$ satisfying the estimates*

$$||u_{\omega}||_{L^{\infty}(0,T;H^1(\Omega))} \leq C_1 \tag{3.13}$$

$$||u_{\omega}||_{L^{\infty}(0,T;L^2(\Omega))} \leq ||u_0||_{L^2(\Omega)} \tag{3.14}$$

$$\left|\left|\frac{\partial u_{\omega}}{\partial t}\right|\right|_{L^2(\Omega)} \leq ||u_0||_{H^1(\Omega)} \tag{3.15}$$

where C_1 is a constant depending only on the constant ν, G_{σ} and $||u_0||_{H^1(\Omega)}$.

Proof: Choosing $v = u_{\omega}$ in (P_w), integrating over the $(0;t)$ and taking into account (3.12) and $u_{\omega}(0) = u_0$, we arrive to the inequality

$$\int_0^t \left(\int_{\Omega} \frac{\partial u_{\omega}(s)}{\partial s} . u_{\omega}(s) dx \right) ds + \nu \int_0^t \int_{\Omega} |\nabla u_{\omega}(t)|^2 \, dx ds \leq 0 \tag{3.16}$$

From (3.16), we deduce that

$$\frac{1}{2} \int_{\Omega} u_w^2(t) \, dx + \nu \int_0^t \int_{\Omega} |\nabla u_w(t)|^2 \, dx \, ds \leq \frac{1}{2} \int_{\Omega} u_0^2 \, dx \tag{3.17}$$

which implies (3.14).

Choosing $v = \partial u_w/\partial t$ in (P_w), we have

$$\int_{\Omega} \left(\frac{\partial u_w}{\partial t} \right)^2 dx + \int_{\Omega} g\left(|(D^{\alpha} G_{\sigma}) * \omega|\right) \nabla u_w(t) . \nabla \left(\frac{\partial u_w(t)}{\partial t} \right) dx = 0. \tag{3.18}$$

Taking into account that

$$\nabla\left(\frac{\partial u_w(t)}{\partial t}\right)=\frac{\partial}{\partial t}\left(\nabla u_w(t)\right) \text{ and } \nabla u_w(t).\frac{\partial}{\partial t}\left(\nabla u_w(t)\right)=\frac{1}{2}\frac{\partial}{\partial t}\left(\nabla u_w(t)\right)^2,$$

we obtain

$$\int_\Omega\left(\frac{\partial u_w(t)}{\partial t}\right)^2 \mathrm{d}x+\frac{1}{2}\int_\Omega g\left(|D^\alpha G_\sigma)*\omega|\right)\frac{\partial|\nabla u_w(t)|^2}{\partial t}\,\mathrm{d}x=0 \tag{3.19}$$

Integrating (3.19) over $(0;t)$, we arrive to that

$$\int_0^t\int_\Omega\left(\frac{\partial u_w(s)}{\partial s}\right)^2 dxds+\frac{1}{2}\int_0^t\int_\Omega g\left(|(D^\alpha G_\sigma)*\omega|\right)\frac{\partial|\nabla u_w(s)|^2}{\partial s}dxds=0 \tag{3.20}$$

Note that

$$\begin{aligned}\int_0^t g\left(\left|\left(D^\alpha G_\sigma\right)*w\right|\right)\frac{\partial|\nabla u_w(s)|^2}{\partial s}ds=&-\int_0^t g'\left(\left|\left(D^\alpha G_\sigma\right)*w\right|\right).\left(\left(D^\alpha G_\sigma\right)*\frac{\partial w}{\partial s}\right).|\nabla u_w(s)|^2\,ds\\&+g\left(\left|\left(D^\alpha G_\sigma\right)*w\right|\right).|\nabla u_w(t)|^2-g\left(\left|\left(D^\alpha G_\sigma\right)*w\right|\right).|\nabla u_0|^2.\end{aligned} \tag{3.21}$$

Inserting (3.21) into (3.20), we obtain

$$\begin{aligned}&\int_0^t\int_\Omega\left(\frac{\partial u_w(s)}{\partial s}\right)^2 dxds+\frac{1}{2}\int_\Omega g\left(|(D^\alpha G_\sigma)*w|\right)|\nabla u_w(t)|^2\,dx\\&=\frac{1}{2}\int_\Omega g\left(|(D^\alpha G_\sigma)*w|\right).|\nabla u_0|^2\,dx\\&+\frac{1}{2}\int_0^t\int_\Omega g'\left(|(D^\alpha G_\sigma)*w|\right).\left(\left(D^\alpha G_\sigma\right)*\frac{\partial w}{\partial s}\right)|\nabla u_w(s)|^2\,dxds.\end{aligned}$$

Since $lim_{s\to\infty}s.g'(s)=0$, there exists a constant $k>0$ such that $s.g'(s)\le k$. Considering moreover that $\left|(D^\alpha G_\sigma)*\frac{\partial w}{\partial s}\right|\le M$ and $1>g\left(|(D^\alpha G_\sigma)*w|\right)\ge\nu$, then

$$\int_0^t\int_\Omega\left(\frac{\partial u_w(s)}{\partial s}\right)^2 dxds+\frac{\nu}{2}\int_\Omega|\nabla u_w|^2\,dx\le\frac{1}{2}\int_\Omega|\nabla u_0|^2\,dx+\frac{Mk}{2}\int_0^t\int_\Omega|\nabla u_w(s)|^2\,dxds \tag{3.22}$$

From (3.17) and (3.22), we note that

$$\int_0^t\int_\Omega\left(\frac{\partial u_w(s)}{\partial s}\right)^2 dxds+\frac{\nu}{2}\int_\Omega|\nabla u_w|^2\,dx\le\frac{1}{2}\int_\Omega|\nabla u_0|^2\,dx+\frac{Mk}{4\nu}\int_\Omega u_0^2dx \tag{3.23}$$

Letting $Mk/(4\nu)\le 1$, yields (3.13) and (3.15).

From proposition 3.1.1, we introduce the subspace W_0 of W, defined by

$$\begin{aligned}W_0=\Big\{w\in W(0,T):w(0)=u_0,||w||_{L^\infty(0,T;H^1(\Omega))}\le C_1,\\||w||_{L^\infty(0,T;H^1(\Omega))}\le||u_0||_{L^2(\Omega)},\left|\left|\frac{dw}{dt}\right|\right|_{L^2(0,T,L^2(\Omega))\times(0,T)}\le||u_0||_{H^1(\Omega)}\Big\}.\end{aligned} \tag{3.24}$$

By construction, $w\to(w)\equiv u_w$ is a mapping from W_0 into W_0. Moreover, one can prove that W_0 is not empty, convex and weakly compact in $W(0,T)$. In order to use the Schauder's fixed-point Theorem, we need to prove that the mapping $S:w\to u_w$ is weakly continuous from W_0 into W_0.

Let w_j be a sequence that converges weakly to some w in W_0 and let $u_j = u_{wj}$. We have to prove that $S(w_j) = u_j$ converges weakly to $S(w) = u_w$. From (3.13)-(3.15) and classical results of compact inclusion in Sobolev space [7], we can extract from w_j a subsequence such that, for some u, we have

$$\begin{aligned}
&\frac{du_j}{dt} \rightarrow \frac{du}{dt}, \text{ weakly in } L^2(\Omega \times (0,T)),\\
&u_j \rightarrow u, \text{ in } L^\infty(0,T;L^2(\Omega)),\\
&\frac{du_j}{dx} \rightarrow \frac{du}{dx}, \frac{du_j}{dy} \rightarrow \frac{du}{dy} \text{ weakly in } L^\infty(0,T;L^2(\Omega)),\\
&w_j \rightarrow w \text{ in } L^\infty(0,T;L^2(\Omega)),\\
&(D_x^\alpha G_\sigma) * w_j \rightarrow (D_x^\alpha G_\sigma) * w \text{ in } L^2(\Omega) (D_y^\alpha G_\sigma) * w_j \rightarrow (D_y^\alpha G_\sigma) * w \text{ in } L^2(\Omega),\\
&g(|(D^\alpha G_\sigma) * w_j|) \rightarrow g(|(D^\alpha G_\sigma) * w|) \text{ in } L^2(0,T;L^2(\Omega)),\\
&u_j(0) \rightarrow u(0), \qquad \text{in} \qquad L^2(\Omega),
\end{aligned}$$

The above convergence allows us to pass to the limit in the problem (P_{wj}) and obtain $u = u_w = S(w)$. Moreover since the solution is unique, the whole sequence $u_j = S(w_j)$ converges weakly in W_0 to $u = S(w)$; that is, S is weakly continuous. Consequently, according to Schauder's fixed-point theorem, there exists $w \in W_0$ such that $w = S(w) = u_w$. The function u_w solves (3.13)-(3.15).

3.1.2 Unicity

Now, we turn to the proof of uniqueness. Let u_1 and u_2 be two solutions of (3.13)-(3.15). For almost every t in $[0,T]$ and $i = 1;2$, we have

$$\frac{\partial u_1}{\partial t}(t) - div[\alpha_1(t)\nabla u_1(t)] = 0 \qquad \frac{\partial u_1}{\partial n}(t) = 0 \qquad u_1(0) = u0, \tag{3.25}$$

$$\frac{\partial u_2}{\partial t}(t) - div[\alpha_2(t)\nabla u_2(t)] = 0 \qquad \frac{\partial u_2}{\partial n}(t) = 0 \qquad u_2(0) = u0, \tag{3.26}$$

where $\alpha_1(t) = g(|(D^\alpha G_\sigma) * u_1|)$ and $\alpha_2(t) = g(|(D^\alpha G_\sigma) * u_2|)$. By using (3.25) and (3.26) and taking into account that the operator $\frac{\partial}{\partial t}$ is linear, we obtain

$$\frac{\partial}{\partial t}(u_1(t) - u_2(t)) - div[\alpha_1(t)(\nabla u_1(t) - \nabla u_2(t)) + (\alpha_1(t) - \alpha_2(t))\nabla u_2(t)] = 0,$$

which implies that

$$\frac{\partial}{\partial t}(u_1(t) - u_2(t)) - div[\alpha_1(t)(\nabla u_1(t) - \nabla u_2(t))] = div[(\alpha_1(t) - \alpha_2(t))\nabla u_2(t)] \tag{3.27}$$

It suffices to show that $u_1 - u_2 \equiv 0$. To verify this, we multiply (3.27) by $u_1(t) - u_2(t)$ to obtain

$$\begin{aligned}
&(u_1(t) - u_2(t))\frac{\partial}{\partial t}(u_1(t) - u_2(t)) - (u_1(t) - u_2(t))div[\alpha_1(t)(\nabla u_1(t) - \nabla u_2(t))]\\
&= (u_1(t) - u_2(t))div[(\alpha_1(t) - \alpha_2(t))\nabla u_1(t))\nabla u_2(t)]
\end{aligned}$$

Applying the method of integration by parts over Ω, we obtain

$$\int_\Omega (u_1(t)-u_2(t))\frac{\partial}{\partial t}(u_1(t)-u_2(t))dx - [(u_1(t)-u_2(t))\alpha_1(t).$$
$$(\nabla u_1(t)-\nabla u_2(t)|_{\partial\Omega} - \int_\Omega \alpha_1(t)(\nabla u_1(t)-\nabla u_2(t))^2 dx)]$$
$$= (\alpha_1(t)-\alpha_2(t)).\nabla u_2.(u_1(t)-au_2(t))|_{\partial\Omega} - \int_\Omega (\alpha_1(t)-\alpha_2(t)).\nabla u_2.(\nabla u_1-\nabla u_2)dx$$

By using the Neumann boundary condition (3.2), we get

$$\int_\Omega (u_1(t)-u_2(t))\frac{\partial}{\partial t}(u_1(t)-u_2(t))dx + \int_\Omega \alpha_1(t)(\nabla u_1(t)-\nabla u_2(t))^2 dx$$
$$= -\int_\Omega (\alpha_1(t)-\alpha_2(t)).\nabla u_2.(\nabla u_1-\nabla u_2)dx. \tag{3.28}$$

Since g is decreasing and positive, it follows that in $(0,T)\times\Omega$, $\alpha i \le \nu$ which implies, from (3.28), that

$$\int_\Omega (u_1(t)-u_2(t))\frac{\partial}{\partial t}((u_1(t)-u_2(t))dx + \nu\int_\Omega (\nabla u_1-\nabla u_2)^2 dx$$
$$\le \int_\Omega (|\alpha_1(t)-\alpha_2(t)|.|\nabla u_1-\nabla u_2|.|\nabla u_2|dx. \tag{3.29}$$

From (3.29), we obtain

$$\frac{1}{2}\frac{d}{dt}\left(||u_1(t)-u_2(t)||^2_{L^2(\Omega)}\right) + \nu||\nabla u_1-\nabla u_2)||^2_{L^2(\Omega)}$$
$$\le ||\alpha_1(t)-\alpha_2(t)||_{L^\infty(\Omega)}.||\nabla u_1-\nabla u_2)||_{L^2(\Omega)}.||\nabla u_2)||^2_{L^2(\Omega)}. \tag{3.30}$$

From Lemma 3.1.1, there exists a positive constant $C>0$ such that

$$||\alpha_1(t)-\alpha_2(t)||_{L^\infty(\Omega)} \le C.||u_1(t)-u_2(t)||_{L^2(\Omega)}. \tag{3.31}$$

In terms of (3.30) and (3.31), we obtain

$$\frac{1}{2}\frac{d}{dt}\left(||u_1(t)-u_2(t)||^2_{L^2(\Omega)}\right) + \nu||\nabla u_1-\nabla u_2)||^2_{L^2(\Omega)}$$
$$\le C.||u_1(t)-u_2(t)||_{L^2(\Omega)}.||\nabla u_1(t)-\nabla u_2(t)||.||\nabla u_2(t)||_{L^2(\Omega)}. \tag{3.32}$$

By using the Young's inequality into (3.32), we obtain

$$\frac{1}{2}\frac{d}{dt}\left(||u_1(t)-u_2(t)||^2_{L^2(\Omega)}\right) + \nu||\nabla u_1(t)-\nabla u_2(t)||^2_{L^2(\Omega)}$$
$$\le \frac{1}{2\nu}C^2.||u_1(t)-u_2(t)||_{L^2(\Omega)}.||\nabla u_2(t)||_{L^2(\Omega)} + \frac{\nu}{2}||\nabla u_1(t)-\nabla u_2(t)||^2_{L^2(\Omega)},$$

from which we deduce

$$\frac{1}{2}\frac{d}{dt}\left(||u_1(t)-u_2(t)||^2_{L^2(\Omega)}\right) \le \frac{1}{\nu}.C^2.||u_1(t)-u_2(t)||^2_{L^2(\Omega)}.||\nabla u_2(t)||^2_{L^2(\Omega)}.$$

Since $u_1(0)=u_2(0)=u_0$, applying Grönwall's inequality (Theorem 1.2.7) yields

$$||u_1(t)-u_2(t)||^2_{L^2(\Omega)} \le 0$$

that is, $u_1=u_2$.

3.2 Numerical schemes

The main purpose of this section is to give an explicit finite difference scheme of the Perona-Malik model with diffusion coeficient depending on fractional gradiant. Before recall the numerical approximation for this model, we will start by discretizing the Caputo-Fabrizio fractional derivative.

3.2.1 Discretization of Caputo-Fabrizio fractional derivative

To solve numerically the fractional Perona-Malik model, we propose to discretize the Caputo-Fabrizio derivative based on the forward finite difference scheme. Taking a partition of N nodes of the interval $[0,x]$, with step $\Delta x = x/N$ and $\alpha \in (0,1)$, then we obtain the numerical approximation of Caputo-Fabrizio derivative based on the forward finite difference scheme in the interval $[0,x]$ (analogously $[0,y]$):

$$\begin{aligned} D_x^{\alpha} u(x_i) &= \frac{1}{1-\alpha}\int_0^{x_i} e^{-(\alpha/(1-\alpha))(x_i-\epsilon)}\, u'(\epsilon)\,\mathrm{d}\epsilon \\ &= \frac{1}{1-\alpha}\sum_{k=0}^{i-1}\int_{x_k}^{x_{k+1}} e^{-(\alpha/(1-\alpha))(x_i-\epsilon)}\, u'(\epsilon_k)\,\mathrm{d}\epsilon \\ &\approx \frac{1}{1-\alpha}\sum_{k=0}^{i-1}\left[\frac{u(x_{k+1})-u(x_k)}{\Delta x}\right]\int_{x_k}^{x_{k+1}} e^{-(\alpha/(1-\alpha))(x_i-\epsilon)}\,\mathrm{d}\epsilon. \end{aligned}$$

Furthermore,

$$\begin{aligned} \int_{x_k}^{x_{k+1}} e^{-(\alpha/(1-\alpha))(x_i-\epsilon)}\mathrm{d}\epsilon &= \frac{1-\alpha}{\alpha}\left[e^{-(\alpha/(1-\alpha))(x_i-\epsilon)}\right]_{x_k}^{x_{k+1}} \\ &= \frac{1-\alpha}{\alpha}\left(e^{-(\alpha/(1-\alpha))(a+i\Delta x-a-(k+1)\Delta x)} - e^{-(\alpha/(1-\alpha))(a+i\Delta x-a-k\Delta x)}\right) \\ &= \frac{1-\alpha}{\alpha}\left(e^{-(\alpha/(1-\alpha))(i-(k+1)\Delta x)} - e^{-(\alpha/(1-\alpha))(i-k)\Delta x)}\right) \\ &= \frac{1-\alpha}{\alpha}e^{-(\alpha/(1-\alpha))(i-k\Delta x)}\left(e^{-(\alpha/(1-\alpha))\Delta x}-1\right) \end{aligned}$$

Thus,

$$D_x^{\alpha} u(x_i) \approx \frac{1}{\alpha\Delta x}\left(e^{-(\alpha/(1-\alpha))\Delta x}-1\right)\sum_{k=0}^{i-1}\left[u(k+1)-u(k)\right]e^{-(\alpha/(1-\alpha))(i-k\Delta x)} \tag{3.33}$$

As in a digital 2D gray image $u(x,y)$, the shortest distance on x and y coordinate is one pixel, then we put $\Delta x = \Delta y = 1$. Therefore, from (3.33), we have

$$\begin{aligned} D_x^{\alpha} u(x_i,y_j) &\approx \frac{1}{\alpha}e^{-\alpha/(1-\alpha)i}\left[e^{\alpha/(1-\alpha)}-1\right]\sum_{k=0}^{i-1} e^{\alpha/(1-\alpha)k}\left[u(k+1,j)-u(k,j)\right] \\ &= \sum_{k=0}^{i-1} C_{\alpha,k}\left[u(k+1,j)-u(k,j)\right], \end{aligned} \tag{3.34}$$

where

$$C_{\alpha,k} = \frac{1}{\alpha}e^{-\alpha/(1-\alpha)i}\left[e^{\alpha/(1-\alpha)}-1\right]e^{\alpha/(1-\alpha)k}$$

An analogue expression is obtained for $D_y^\alpha u(x_i, y_j)$,

$$D_y^\alpha u(x_i, y_j) \approx \frac{1}{\alpha} e^{-\alpha/(1-\alpha)j} \left[e^{\alpha/(1-\alpha)} - 1\right] \sum_{k=0}^{j-1} e^{\alpha/(1-\alpha)k} \left[u(i, k+1) - u(i, k)\right]$$
$$= \sum_{k=0}^{j-1} C_{\alpha,k} \left[u(i, k+1) - u(i, k)\right], \tag{3.35}$$

Now putting the function G_σ into (3.34) and (3.35), respectively, we obtain

$$D_x^\alpha G_\sigma(x_i, y_j) = \sum_{k=0}^{i-1} C_{\alpha,k}. \left[G_\sigma(k+1, j) - G_\sigma(k, j)\right], \tag{3.36}$$

and

$$D_y^\alpha G_\sigma(x_i, y_j) = \sum_{k=0}^{j-1} C_{\alpha,k}. \left[G_\sigma(i, k+1) - G_\sigma(i, k)\right]. \tag{3.37}$$

Considering that

$$G_\sigma(k, j) = \frac{1}{\sqrt{2\pi\sigma}} e^{-\frac{1}{4\sigma}(k^2+j^2)}$$
$$G_\sigma(k+1, j) = \frac{1}{\sqrt{2\pi\sigma}} e^{-\frac{1}{4\sigma}((k+1)^2+j^2)}$$
$$G_\sigma(i, k) = \frac{1}{\sqrt{2\pi\sigma}} e^{-\frac{1}{4\sigma}(i^2+k^2)}$$
$$G_\sigma(i, k+1) = \frac{1}{\sqrt{2\pi\sigma}} e^{-\frac{1}{4\sigma}(i^2+(k+1)^2)}$$

we obtain from (3.36) and (3.37)

$$D_x^\alpha G_\sigma(x_i, y_j) \approx \sum_{k=0}^{i-1} C_{\sigma,\alpha,k} \left[e^{-\frac{1}{4\sigma}((k+1)^2+j^2)} - e^{-\frac{1}{4\sigma}(k^2+j^2)}\right], \tag{3.38}$$

and

$$D_y^\alpha G_\sigma(x_i, y_j) \approx \sum_{k=0}^{j-1} C_{\sigma,\alpha,k} \left[e^{-\frac{1}{4\sigma}(i^2+(k+1)^2)} - e^{-\frac{1}{4\sigma}(i^2+k^2)}\right], \tag{3.39}$$

respectively. Where the coefficients $C_{\sigma,\alpha,k}$ are given by

$$C_{\sigma,\alpha,k} = \frac{1}{\sqrt{2\pi\sigma}}.C_{\alpha,k}.$$

3.2.2 Numerical scheme of the model

Denoting u_{kj}^n an approximation of $u(k, j, n\Delta t)$. We put:

$$\alpha_{kj}^n \approx g(|(D^\alpha G_\sigma(x, y)) * u(x, y, t)|)(k, j, n\Delta t).$$

Then we discretize:

$$g(|(D^\alpha G_\sigma(x, y)) * u(x, y, t)|)\partial u(x, y, t)/\partial x \approx \alpha_{k,j}^n \partial u(x, y, t)/\partial x(k, j, n\Delta t)$$

and

$$\partial/\partial x\left[g(|(D^{\alpha}G_{\sigma}(x,y))*u(x,y,t))\partial u(x,y,t)/\partial x\right]$$
$$\approx \frac{1}{2\Delta x^2}[(\alpha^n_{k-1,j}+\alpha^n_{k,j})u^n_{k-1,j}-(2\alpha^n_{k,j}+\alpha^n_{k-1,j}+\alpha^n_{k+1,j})u^n_{k,j}+(\alpha^n_{k,j}+\alpha^n_{k+1,j})u^n_{k+1,j}] \tag{3.40}$$

Similarly for

$$\partial/\partial y\left[g(|(D^{\alpha}G_{\sigma}(x,y))*u(x,y,t))\partial u(x,y,t)/\partial y\right]$$
$$\approx \frac{1}{2\Delta y^2}[(\alpha^n_{i,k-1}+\alpha^n_{i,k})u^n_{i,k-1}-(2\alpha^n_{i,k}+\alpha^n_{i,k-1}+\alpha^n_{i,k+1})u^n_{i,k}+(\alpha^n_{i,k}+\alpha^n_{i,k+1})u^n_{i,k+1}] \tag{3.41}$$

By adding (3.40) and (3.41), and putting $\Delta x=\Delta y=h$ we obtain

$$\begin{aligned}&\frac{1}{2h^2}[(\alpha^n_{k-1,j}+\alpha^n_{k,j})u^n_{k-1,j}+(\alpha^n_{k,j-1}+\alpha^n_{k,j})u^n_{k,j-1}\\&+(\alpha^n_{k,j}+\alpha^n_{k+1,j})u^n_{k+1,j}+(\alpha^n_{k,j}+\alpha^n_{k,j+1})u^n_{k,j+1}\\&-(4\alpha^n_{k,j}+\alpha^n_{k-1,j}+\alpha^n_{k+1,j}+\alpha^n_{k,j-1}+\alpha^n_{k,j+1})u^n_{k,j}]\end{aligned} \tag{3.42}$$

Finally, we obtain the explicit numerical scheme

$$\begin{aligned}&\frac{u^{n+1}_{k,j}-u^n_{k,j}}{\Delta t}-\frac{1}{2h^2}[(\alpha^n_{k-1,j}+\alpha^n_{k,j})u^n_{k-1,j}+(\alpha^n_{k,j-1}+\alpha^n_{k,j})u^n_{k,j-1}\\&+(\alpha^n_{k,j}+\alpha^n_{k+1,j})u^n_{k+1,j}+(\alpha^n_{k,j}+\alpha^n_{k,j+1})u^n_{k,j+1}\\&-(4\alpha^n_{k,j}+\alpha^n_{k-1,j}+\alpha^n_{k+1,j}+\alpha^n_{k,j-1}+\alpha^n_{k,j+1})u^n_{k,j}]=0\end{aligned} \tag{3.43}$$

3.2.3 Experimental results

In this section, we will talk about how the model (3.1) affects various gray scale images. We will also compare the results for different values of the fractional derivative order α, and explain how well the model improves edges and reduces noise. All experiments were done using the explicit numerical scheme (3.43) with $h=1$ and $\delta t=1/4$.

The images in Figure (3.1) show the effects of diffusion at different values of the fractional derivative order α. Figure (3.2) shows a comparison of smoothed images obtained by the fractional Perona-Malik model and Catté and al's. model.

The second simulation concerned the efficacy of the model (3.1) in reducing noise. Figure (3.3) show how noise reduction and edge preservation can be combined using this model.

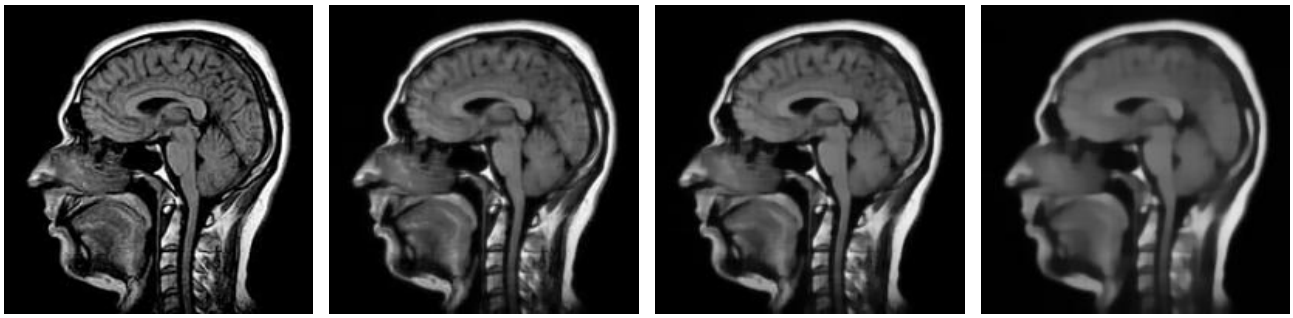

(a) (b) (c) (d)

Figure 3.1: Comparison of different filtering models after 10 iterations. From left to right: original images, smoothed original image by the fractional Perona-Malik model for $\alpha = 0.1, 0.5, 0.9$, respectively.

(a) (b) (c)

Figure 3.2: Comparison of different filtering models after 20 iterations. From left to right: original images, smoothed original image by the fractional Perona-Malik model for $\alpha = 0.1$ and smoothed original image by Catté and al. model, respectively.

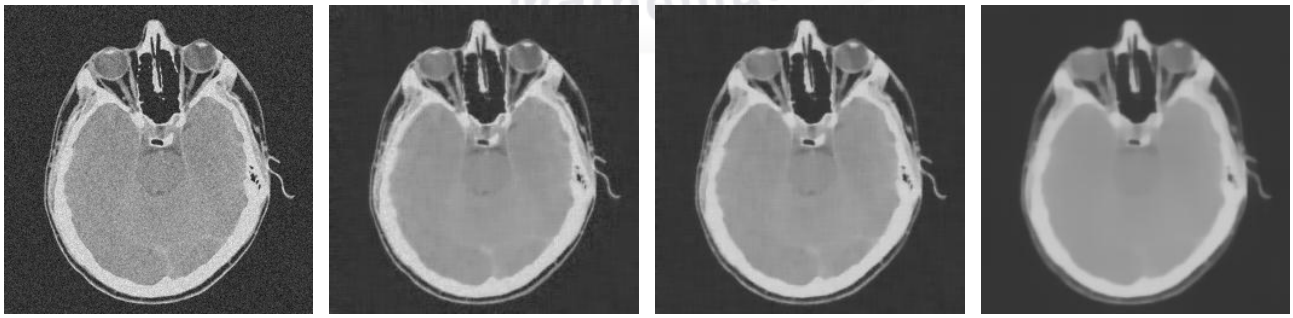

(a) (b) (c) (d)

Figure 3.3: Comparison of different filtering models after 10 iterations. From left to right: original noisy images, denoised original image by the fractional Perona-Malik model for $\alpha = 0.5$ and denoised original image by Catté and al. model, respectively.

Conclusion

In this work, we first introduced the famous PDEs that appear in the field of image processing, starting with the heat diffusion equation as a linear filter. The linear diffusion filter has its limitations: the process not only removes undesirable local extrema (noise) but also deforms important features of the image, blurs, and dislocates edges. To overcome these drawbacks, we need to move to nonlinear filters. The nonlinear diffusion model, particularly the Perona-Malik model, offers an excellent alternative. This technique not only preserves edge sharpness but may also enhance it. However, the Perona-Malik model has several practical and theoretical difficulties. Among them, for example, are ensuring both the existence and uniqueness of solutions; certain conditions must be met. If these conditions are not satisfied, Perona and Malik's equation will be an ill-posed problem. The model proposed by Catté et al. [5] synthesizes Perona and Malik's ideas while avoiding the drawbacks of their model.

Secondly, we presented a fractional diffusion model, which is a modified version of the Perona-Malik model, by introducing the Caputo-Fabrizio fractional gradient inside the diffusivity function. A theoretical study examining the existence and uniqueness of the solution was conducted. In addition, we conducted a numerical study that allowed us to perform experiments to confirm the effectiveness of this model for noise reduction and edge preservation. This also enabled us to compare the obtained results with those of the classical Perona-Malik model.

Bibliography

[1] L. Alvarez, F. Guichard, P.L. Lions and J.M. Morel, Axioms and fundamental equations of image processing, Archive for Rational Mechanics and Analysis. (1993) Vol. 123, pp. 199-257.

[2] M. Bertero,T.A Poggio and V. Torre, Ill-posed problems in early vision. Proceedings of the IEEE. (1988) Vol. 76, pp. 869-889.

[3] H. Brezis, Functional Analysis, Sobolev Spaces, and Partial Differential Equations, New York: Springer, (2010).

[4] R.W. Brockett and P. Maragos, Evolution equations for continuous-scale morphological filtering, IEEE Transactions on Signal Processing, (1994) Vol. 42, pp. 3377-3386.

[5] F. Catté, P. Lions, J. Morel and T. Coll, Image Selective Smoothing and Edge Detection by Nonlinear Diffusion, Siam Journal on Numerical Analysis (1992), vol. 29, pp. 182-193.

[6] M. Caputo and M. Fabrizio, A new Definition of Fractional Derivative without Singular Kernel, Progr. Fract. Differ. Appl. (2015) vol. 1, no. 2, pp. 1-13.

[7] L. C. Evans, Partial Differential Equations. American Mathematical Society (1997), Vol. 19, pp.349-364.

[8] T. Iijima, Basic equation of figure and observational transformation, Systems Computers, (1971) Vol. 4, pp. 70-77 .

[9] J. Koenderink, The structure of images, Biol. Cybern (1984), Vol.50, pp.363-370.

[10] P. Kornprobst and G, Aubert, Mathematical problems in Image processing :Partial Differential Equations and the Calculus of Variations. new york, berlin, heidelberg, hong kong, london, milan, paris, tokyo, (2002).

[11] E. Lieb and M. Loss, Analysis, American Mathematical Society (2001), vol. 14.

[12] R. Malladi and J.A. Sethian, Image Processing: Flows under Min/ Max curvature and Mean Curvature, Graphical Models and Image Processing, (1996) Vol. 58, pp. 127-141.

[13] G. A. Mboro-Nchama, A. L. Mecías and M. R. Ricard, A New Version of Catté-Lions-Morel Model for Image Smoothing and Edge Detection, Global Journal of Pure and Applied Mathematics, (2020), Vol.16, No. 6, pp. 819-842.

[14] P. Perona and J. Malik, Scale space and edge detection using anisotropic diffusion, in Proc. IEEE Computer Society Workshop on Computer Vision, (1987).

[15] C.B. Schonlieb, Partial Differential Equation Methods for Image Inpainting, Cambridge University Press, (2015) Vol. 29.

[16] R. Van den Boomgaard and A. Smeulders, The morphological structure of images : The differential equations of morphological scale-space, IEEE Transactions on Pattern Analysis and Machine Intelligence, (1994) Vol. 16, pp. 1101-1113.

[17] J. Weickert, Anisotropic Diffusion in Image Processing. Ph. D. Thesis, Kaiserslautern University, (1996).

[18] M. Welk, M. Breu and O. Vogel, Morphological amoebas are self-snakes, Journal of Mathematical Imagin and Vision, (2011) Vol. 39, pp. 87-99.

[19] A.P. Witkin, Scale-space filtering, Presented at 8th int. Joint conf. Art. intell., Karlsruhe, Germany (1983)

Abstract

This work presents a fractional diffusion model, which modifies the Perona-Malik model by incorporating the Caputo-Fabrizio fractional gradient into the diffusivity function. A theoretical investigation was conducted to examine the existence and uniqueness of the solution. Additionally, we carried out a numerical study, enabling us to perform experiments that confirmed the model's effectiveness in noise reduction and edge preservation. This also allowed us to compare our results with those of the classical Perona-Malik model.
Key words: Image processing, Linear and non-linear diffusion, Existence, Uniqueness, Caputo-Fabrizio fractional derivative, Finite difference approximations.

Résumé

Ce travail présente un modèle de diffusion fractionnaire, qui modifie le modèle de Perona-Malik en incorporant le gradient fractionnaire de Caputo-Fabrizio dans la fonction de diffusivité. Une étude théorique a été menée pour examiner l'existence et l'unicité de la solution. De plus, nous avons réalisé une étude numérique qui nous a permis de mener des expériments confirmant l'efficacité de ce modèle pour la réduction de bruit et la préservation des contours. Cela nous a également permis de comparer les résultats avec ceux du modèle classique de Perona-Malik.
Mots-clés: Traitement d'image, Diffusion linéaire et non linéaire, Existence, Unicité, Dérivée fractionnaire de Caputo-Fabrizio, Approximations aux différences finies.

ملخص

يتناول هذا العمل عرض نموذج انتشار كسري ، يعدل نموذج بيرونا – ماليك من خلال دمج التدرج الكسري لكابوتو – فابريزيو داخل دالة الانتشار. تم إجراء دراسة نظرية تتضمن فحص وجود الحل وحدانيته. بالإضافة إلى ذلك، قمنا بإجراء دراسة رقمية مكنتنا من إجراء تجارب أكدت فعالية هذا النموذج في تقليل الضوضاء والحفاظ على الحواف. كما سمح لنا ذلك بمقارنة النتائج التي تم الحصول عليها مع نتائج نموذج بيرونا – مالك الكلاسيكي.
الكلمات المفتاحية:
معالجة الصور، الانتشار الخطي وغير الخطي، وجود الحل وحدانيته، مشتقات كابوتو – فابريزيو الكسرية، تقريب الفروق المتهية.